Life Sciences 225 (2019) 55–63

Contents lists available at ScienceDirect

Life Sciences

journal homepage: www.elsevier.com/locate/lifescie

Activation of KRas-ERK1/2 signaling drives the initiation and progression of glioma by suppressing the acetylation of histone H4 at lysine 16

Yuzhen Wei[a,b,1], Fang Wang[c,1], Ben Sang[a], Zhen Xu[a], Dongxu Yang[d,*]

[a] Department of Neurosurgery, Jining No.1 People's Hospital, Jining 272011, China
[b] Affiliated Jining NO.1 People's Hospital of Jining Medical University, Jining Medical University, Jining 272067, China
[c] Department of Pathology, Jining No.1 People's Hospital, Jining 272011, China
[d] Department of Neurosurgery, Affiliated Hospital of Jining Medical University, Jining 272000, China

ARTICLE INFO

Keywords:
Glioma
Acetylation of H4 at lysine 16 (H4K16ac)
KRas-ERK1/2 signaling
Sirt2
TIP60

ABSTRACT

Background/Aims: Acetylation of H4 at lysine 16 (H4K16ac) has been well-characterized as an acetylated mark, and the expression of which is closely associated with the tumorigenesis of human cancers. This study aimed to reveal whether KRas mutation drives the initiation and progression of glioma via modulation of H4 acetylation.
Methods: Changes of H4K16 acetylation in human glioblastoma A172 cells following transfection with a plasmid for expression of mutant KRas were tested by western blot analysis. MTT assay, transwell assay, soft-agar colony formation assay, RT-PCR and chromatin immunoprecipitation were carried out to evaluate the effect of H4K16ac on A172 cells growth and migration. Furthermore, the enzymes participating in the deacetylation of H4K16ac were studied by using RT-PCR and western blot analysis.
Results: H4K16ac was found to be deacetylated by KRas-ERK1/2 activation. H4K16Q (a plasmid for mimicking H4K16ac) repressed A172 cells viability, colony formation, and migratory capacity. Besides, H4K16ac was capable of regulating the transcription of several ERK1/2 pathway downstream genes. KRas-ERK1/2 signaling repressed H4 acetylation at K16 via modulation of a histone deacetylase Sirt2, as well as a histone acetyltransferase TIP60. Moreover, KRas-ERK1/2 inhibited TIP60 via an MDM2-dependnet fashion.
Conclusion: Our results suggest that activation of KRas-ERK1/2 signaling participates in the onset and progression of glioma at least partially through modulating acetylation of H4 at K16. KRas-ERK1/2 signaling mediates the acetylation of H4K16 via Sirt2 and MDM2-dependnet degeneration of TIP60.

1. Introduction

Glioma is the most common, aggressive and lethal intracranial brain tumor, which accounts for about 80% of all malignant tumors in brain [1]. Glioma grows in an infiltrating model, which makes it extremely malignancy with an average median survival < 1 year [2]. Despite significant improvement of glioma management has been achieved in recent years, including surgery, radiotherapy, chemotherapy, immunotherapy as well as gene therapy [3], glioma remains incurable and glioma treatment has always been the medical challenges faced by the neurosurgeon all around the world [4]. A better understanding of glioma pathogenesis will be helpful for further improvement of glioma treatment.

Ras is the first identified proto-oncogene that is closely associated with human tumors. Ras protein is encoded by three ubiquitously expressed genes, i.e., *HRas*, *KRas*, and *NRas* which are located at chromosome 11p15.5, 1p13, and 12p12.1 with DNA lengths of 3, 35 and 7 kb, respectively. It has been widely accepted that *Ras* mutation is an initial process occurs in the onset of multiple human tumors, including glioma [5]. Approximately 17% of cancer patients harbor an activated *Ras* mutation [6,7]. Besides, *Ras* mutation acts as a switch in activation of several signaling, including PI3K, MEK and ERK [8]. In vivo study has shown that mutant *KRas* increases tumor incidence in glial progenitor cells and allows gliomagenesis from astrocytes [9]. Taken together, these previous studies suggested the inductive effects of *KRas* mutation in gliomagenesis. The activated signaling by *KRas* mutation can be a contributing factor to the predominance of *KRas* mutation in glioma. However, how KRas-ERK signaling participates in the onset and progression of glioma is still unclear.

Epigenetics is a subject which has been identified as heritable changes in gene expression that are not attributable to any alteration in DNA sequences. Aberrant DNA methylation, histone modification and

* Corresponding author at: Department of Neurosurgery, Affiliated Hospital of Jining Medical University, No.89 Guhuai Road, Jining 272000, China.
E-mail address: yangdongxu0040@sina.com (D. Yang).
[1] Co-first authors.

https://doi.org/10.1016/j.lfs.2019.03.079
Received 12 December 2018; Received in revised form 23 March 2019; Accepted 31 March 2019
Available online 01 April 2019

miRNA post-transcriptional regulation have all been recognized as epigenetic modifications [10]. Among which, it has been widely accepted that histone modification is one of the major causes of human cancer initiation and progression [11]. H1, H2A, H2B, H3 and H4 are five subunits of histone. Histone H4 is a highly-conserved protein and lysine acetylation at the N-terminus tails of H4 is classically associated with gene expression [12]. Acetylation of H4 at lysine 16 (H4K16ac) has been well-characterized as an acetylated mark that is particularly enriched at transcriptionally active gene promoters [13]. Of note, it has been shown that, H4K16ac is closely associated with the tumorigenesis of several cancers [14,15].

This study aimed to reveal whether *KRas* mutation drives tumorigenesis via modulation of H4 modification. To this end, the gene of *KRas* in human glioblastoma cell line A172 was mutated at G12V and T35S, and thus the changes in H4K16 acetylation were monitored. Besides, how KRas-ERK signaling altered H4K16 acetylation was studied. This study will reveal a new insight into the involvement of KRas-ERK signaling in glioma through the study from the perspective of histone modification.

2. Martials and methods

2.1. Plasmid construction and transfection

The 3′untranslated region (3′UTR) of *H4*, wild type of *Ras* (Ras^{WT}), *Sirt2*, *TIP60* and *MDM2* was amplified by PCR. The amplified *H4* and *Ras* sequences were inserted into pEGFP-N1 plasmid (Clontech, Palo Alto, CA). The PCR produces with sequences of *Sirt2* and *TIP60* were subcloned into HA-tagged vector (EK-Bioscience, Shanghai, China). The PCR produces with sequences of *MDM2* were subcloned into His-tagged vector (Invitrogen, Carlsbad, CA). The pEGFP-$Ras^{G12V/T35S}$ construct and MDM2-MU-His were mutated using site-directed mutagenesis. The pEGFP-H4K16Q plasmid was constructed using the MutanBEST Kit (TaKaRa, Dalian, China) for mimicking *H4K16ac*. The small interfering RNAs (siRNAs) specific for *Sirt2* and *MDM2* were purchased from GenePharma (Shanghai, China). The non-targeting sequence served as a negative control (si-con.). pc-TIP60 plasmid for expression *TIP60* was constructed by inserting *TIP60* into pcDNA-3.1 vector (GenePharma).

All plasmids were transfected into cell with the mediation of Lipofectamine 2000 (Invitrogen) under serum-free and antibiotics-free conditions in 6-well plates. After 48 h of transfection, the culture medium was refreshed by the medium containing G418 (Gibco, Grand Island, NY) for selecting stable transfectants.

2.2. Cell culture and treatments

Human glioblastoma cell line A172 purchased from Cell Bank of Chinese Academy of Science (Shanghai, China) was cultured in DMEM medium (Gibco) containing 1.5 g/L $NaHCO_3$ (Sangon Biotech, Shanghai, China), and 10% fetal bovine serum (FBS, Gibco). The cells were routinely cultured in 75 cm^2 flasks at 37 °C under humidified atmosphere with 5% CO_2. SCH772984, a specific inhibitor of ERK1/2 purchased from Selleck Chemicals (Houston, TX) was utilized to treat cell at concentration of 1 μM for 5 h.

2.3. Cell viability

After the indicated transfection, cells were seeded in 96-well plates (5000 cells per well) and incubated at 37 °C for 48 h. Thiazolyl blue tetrazolium bromide (MTT) purchased from (Sangon Biotech) with a final concentration of 5 mg/mL was added to each well, and the plates were incubated at 37 °C for another 4 h. Thereafter, MTT reagent was removed from the plates, and 150 μL dimethyl sulfoxide (DMSO, Sigma-Aldrich, St. Louis, MO) was added to dissolve the formazan crystals. The optical density (OD) of each sample was measured by a Microplate reader (Bio-Rad Laboratories, Hercules, CA) at 490 nm.

2.4. Soft-agar colony formation assay

6-well plates were pre-coated with 0.6% low-melting agarose (Solarbio, Beijing, China) at 4 °C until the agarose was solidified. The transfected cells were collected and the cell suspension was added into each well (500 cells/well) in combination with 1 mL 0.35% low-melting agarose. After 2 weeks incubation at 37 °C, the number of colonies was counted microscopically (40 ×).

2.5. Transwell assay

The transfected cells were collected and suspended in serum-free medium. The cell suspension was added to the upper chamber of the 24-well transwell system (8-μm pore filter, Costar, Boston, MA). Culture medium containing 10% FBS was added into the lower chamber of the transwell system. After 24 h of incubation at 37 °C, the cells in the lower side were stained with 0.1% crystal violet (Sangon Biotech). 0.1 mL 33% acetic acid (Sangon Biotech) was used for decolorization, and the OD values of each sample were measured by the Microplate reader (Bio-Rad Laboratories) at 570 nm.

2.6. Assessment of cell cycle progression

The cell cycle distribution was detected by using Fluorimetric Cell Cycle Assay Kit (Sangon Biotech). Briefly, the collected cells after transfection were suspended in pre-heated medium with a concentration of 5×10^5 cells/mL. 2.5 μL 200 × Nuclear Green™ LCS1 was added and the sample was incubated at 37 °C for 30 min. The cells were collected by centrifugation at 1200*g* for 4 min, and then cells were re-suspended in 0.5 mL Assay Buffer. The distribution of cell in G0/G1, S and G2/M phases was measured by a flow cytometer (Beckman Coulter, Fullerton, CA).

2.7. RNA extraction and real-time polymerase chain reaction (RT-PCR)

After the indicated transfection, total RNAs were extracted from cell by using TRIzol reagent (Invitrogen). Complementary DNA (cDNA) was synthesized using Transcriptor First Strand cDNA Synthesis Kit (Roche, Basel, Switzerland). RT-PCR was carried out by using FastStart Universal SYBR Green Master (Roche). The amounts of targeted mRNAs were standardized against β-actin. Data were analyzed according to the classic $2^{-\Delta\Delta Ct}$ method. Primary sequences used were listed in Table 1.

Table 1
The sequence of primers used in RT-PCR.

	Primers
Sirt2	Forward, 5′-CATCCACCGGCCTCTATGAC-3′ Reverse, 5′-CCAGCTTAGCGGGTATTCGT-3′
TIP60	Forward, 5′-GGCACAACTCA- GAACTCACAAG-3′ Reverse, 5′-ACTCATCTTCGTTGTCCTGGTTG-3′
CYR61	Forward, 5′-CCAGTGTACAGCAGCCTGAA-3′ Reverse, 5′-GCCTGTAGAAGGGAAACGCT-3′
IGFBP3	Forward, 5′-CTGATCCCAAGTTCCACCCC-3′ Reverse, 5′-GGGAATGTGTACACCCCTGG-3′
WNT16B	Forward, 5′-CCCTATGGTGGTTGGGCATT-3′ Reverse, 5′-TCTTGCACAGCTCCTTCTGG-3′
NT5E	Forward, 5′-GTATCCGGTCGCCCATTGAT-3′ Reverse, 5′-CCGACCTTCAACTGCTGGAT-3′
GDF15	Forward, 5′-GCAAGAACTCAGGACGGTGA-3′ Reverse, 5′-TGGAGTCTTCGGAGTGCAAC-3′
CARD16	Forward, 5′-GTGCAGGACAACCCAGCTAT-3′ Reverse, 5′-GTTCCTCCAGAACCGCTCAA-3′
β-actin	Forward, 5′-CCGTTGCCCTGAGGCTCTTT-3′ Reverse, 5′-TGTCAGCAATGCCAGGGTACAT-3′

2.8. Western blot

Total protein was isolated from the transfected cells by using RIPA lysis buffer (Beyotime, Shanghai, China) over ice for 30 min. BCA Protein Assay Kit (Novagen, Madison, WI) was used for testing the purity of the protein extracts. Equal amounts of the protein were separated by sodium dodecyl sulfate (SDS)-polyacrylamide gel (PAGE) and transferred on to polyvinylidene fluoride (PVDF) membranes (Millipore, Bedford, MA). After blocking and rinsing, the proteins in membranes were probed with the primary antibodies for 12 h at 4 °C. The primary antibodies and corresponding dilutions used were as follows: anti-p-ERK1/2 (ab214362, 1:500), anti-ERK1/2 (ab54230, 1:500), anti-H4K16ac (ab109463, 1:1000), anti-H4 (ab10158, 1:1000), anti-HA (ab137838, 1:1000), anti-GFP (ab6556, 1:2000), anti-TIP60 (ab151432, 1:2000), anti-β-actin (ab8227, 1:1000), anti-His (ab27025, 1:1000) and anti-MDM2 (ab38618, 1:1000, all from Abcam, Cambridge, MA). The membranes were then incubated with goat anti-rabbit IgG (ab7079, 1:5000) and goat-anti-mouse IgG (ab97040, 1:5000, both from Abcam) for 1 h at room temperature. Positive bands were enhanced by enhanced chemiluminescent (ECL) method, and the intensity of each bands were analyzed by using Image Lab™ Software (Bio-Rad Laboratories).

2.9. Chromatin immunoprecipitation (ChIP)

The transfected cells were collected and fixed with 1% formaldehyde (Sangon Biotech). The DNA and proteins in cell were cross-linked with each other. The cells were then washed twice with ice-cold phosphate buffer saline (PBS), and lysed with SDS lysis buffer (Beyotime). The lysates were sonicated in an ultrasonic bath (HuaRui BoYuan Technology Co., LTD, Beijing, China). The samples were centrifuged at 15,000*g* for 5 min, and the supernatants were collected for use in immunoprecipitation. The primary antibodies specific against H4K16ac (Biorbyt, San Francisco, CA) and TIP60 (United States Biological, Salem, MA) were used in this process. Anti-IgG antibody (Abcam, Cambridge, MA) was used as a negative control. After washing with gradient salt solution, the DNA was eluted from the beads and the immunoprecipitated DNA was analyzed by RT-PCR. Primary sequences used were listed in Table 2.

2.10. Statistical analysis

Data presented as mean ± standard deviation (SD) from three independent experiments. Statistical analyses were done by using one way ANOVA following Duncan post-hoc test in SPSS 19.0 software (Chicago, IL). A *P*-value < 0.05 was considered to indicate the significant result.

Table 2
The sequence of primers used in ChIP.

	Primers
CYR61	Forward, 5′-TCAACGAGGACTGCAGCAAA-3′
	Reverse, 5′-CTGCAGATCCCCTTCAGAGC-3′
IGFBP3	Forward, 5′-TGCCTGGATTCCACAGCTTC-3′
	Reverse, 5′-CTGCATGACGCCTGCAAC-3′
WNT16B	Forward, 5′-GGAGCAGAAGAGGAAGAGCC-3′
	Reverse, 5′-CAGCATGGGAATGCATCAGC-3′
NT5E	Forward, 5′-GAGCTAGCGCAACCACAAA-3′
	Reverse, 5′-TGGGTCCTCTCTGAGTCTCG-3′
GDF15	Forward, 5′-TCAGAGCCGCAACCTGC-3′
	Reverse, 5′-GCAACACCAGGAGCATCTGA-3′
CARD16	Forward, 5′-TCCATTCCATGGGTGAAGGT-3′
	Reverse, 5′-CTGGTTCAGCACCCTTGTCT-3′

3. Results

3.1. KRas-ERK1/2 activation regulates the acetylation of H4 at K16

pEGFP-Ras$^{G12V/T35S}$ construct for expression of the mutant type of *KRas* was transfected into A172 cells. As a result, the expression of phosphorylated ERK1/2 was significantly up-regulated after transfection with pEGFP-Ras$^{G12V/T35S}$, as compared to transfection with an empty pEGFP vector ($P < 0.05$, Fig. 1). Next, the expression changes of H4 were tested to see if the activation of ERK1/2 signaling induced by Ras$^{G12V/T35S}$ could alter H4 modification. Results from western blot revealed that, the expression level of H4K16ac was significantly reduced by pEGFP-Ras$^{G12V/T35S}$ transfection, as compared to those in pEGFP and Ras^{WT} transfected cells ($P < 0.05$, Fig. 1B). It seems that ERK1/2 activation induced by Ras$^{G12V/T35S}$ represses the acetylation of H4 at K16.

3.2. H4K16ac inhibits A172 cells survival and migration

It is well-known that, KRas-ERK1/2 is a key signaling in driving tumor cells growth and metastasis. Herein, we determined the effects of H4K16ac on A172 cells survival and migration when KRas-ERK1/2 was activated. To this end, H4K16Q construct for expression of mimicked H4K16ac was transfected into A172 cells. Results in Fig. 2A displayed that, the viability of A172 cells was significantly declined with the increasing amounts of H4K16Q ($P < 0.05$), suggesting the anti-proliferative role of H4K16ac in A172 cells. Considering 2 g of H4K16Q plasmid resulted in the minimum cell viability, 2 g was selected as the optimal amount for use in the following transfection. Soft-agar colony formation assay results indicated that transfection of cells with H4K16Q significantly decreased the number of colonies, as compared to transfection with H4 ($P < 0.05$, Fig. 2B). Same trends were observed from Transwell assay ($P < 0.05$, Fig. 2C). These data collectively suggested that H4 acetylation at K16 has capacities in suppressing A172 cells survival and migration.

3.3. H4K16ac participates in regulating ERK1/2 pathway downstream genes

To further link H4K16ac with KRas-ERK1/2 signaling induced response, the regulatory effects of H4K16ac on the transcription of ERK1/2 pathway downstream genes were evaluated. RT-PCR data in Fig. 3A revealed that, mRNA levels of *CYR61*, *IGFBP3* and *WNT16B* were significantly down-regulated whereas the mRNA levels of *NT5E*, *GDF15* and *CARD16* were significantly up-regulated by H4K16Q transfection ($P < 0.05$, Fig. 3A). Besides, data from ChIP indicated that the enrichment of H4K16ac was significantly declined by the promoter of the abovementioned genes ($P < 0.05$, Fig. 3B). All these suggested that, H4K16ac could mediate the transcription of ERK1/2 pathway downstream genes.

3.4. KRas-ERK1/2 signaling repressed H4K16ac via modulation of Sirt2

It has been previously reported that histone deacetylase Sirt2 has a strong preference for H4K16ac in its deacetylation activity [16]. The present work attempted to reveal whether KRas-ERK1/2 signaling induced the deacetylation of H4K16ac via modulating Sirt2. To this end, the expression of Sirt2 in A172 cells was silenced by siRNAs transfection. Fig. 4A showed that, the mRNA levels of Sirt2 were dramatically suppressed after transfection with two sequences of siRNAs (si-Sirt2-1 and si-Sirt2-2). Besides, we found that Sirt2 silence recovered H4K16ac expression even when KRas-ERK1/2 was activated, while it did not recover H4K16ac expression in the presence of ERK1/2 specific inhibitor SCH772984 ($P < 0.05$, Fig. 4B). The results indicated that KRas-ERK1/2 signaling repressed H4 acetylation at K16 via modulation of Sirt2. Further experiments revealed that Sirt2 silence exhibited a

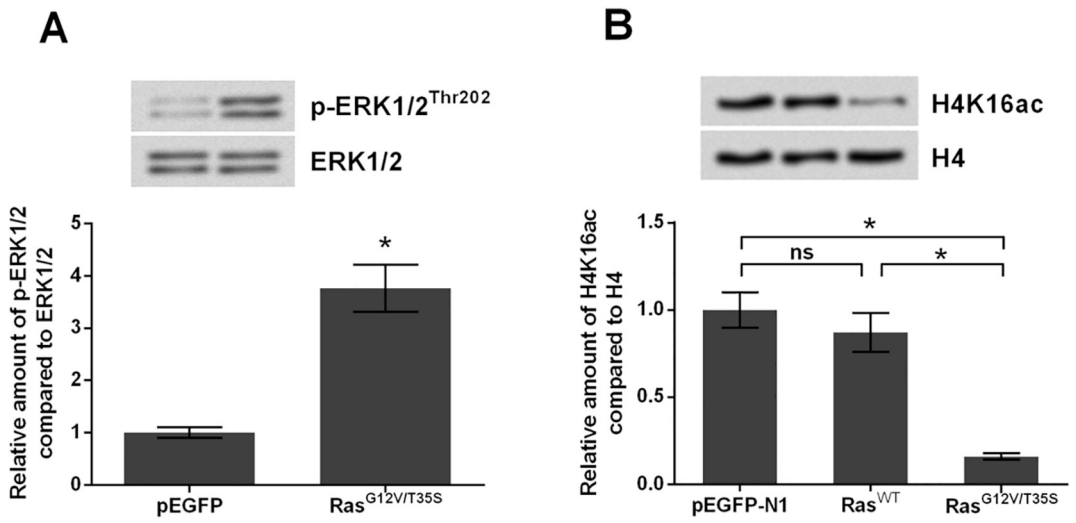

Fig. 1. KRas-ERK1/2 activation regulates the acetylation of H4 at K16. (A) ERK1/2 was remarkably phosphorylated at Thr202 after A172 cells were transfected with pEGFP-Ras$^{G12V/T35S}$ plasmid, as compared to transfection with an empty pEGFP-N1 vector. (B) Transfection of cells with pEGFP-Ras$^{G12V/T35S}$ significantly reduced the expression of H4K16ac, as compared to transfection with pEGFP-Ras^{WT} or pEGFP-N1. ns, no significance; *, $P < 0.05$ vs. the indicated group.

similar effect as H4K16Q on A172 cells growth and migration. As shown in Fig. 4C–E, transfection of cells with si-Sirt2 significantly reduced A172 cells viability ($P < 0.05$), S phase arrest, and relative migration ($P < 0.05$). Not surprisingly, the mRNA levels of *CYR61*, *IGFBP3* and *WNT16B* were significantly down-regulated whereas the mRNA levels of *NT5E*, *GDF15* and *CARD16* were significantly up-regulated by si-Sirt2 transfection ($P < 0.05$, Fig. 4F). Thus, it might be rational that H4K16ac functioned to A172 cells via a Sirt2-dependent fashion.

3.5. KRas-ERK1/2 signaling repressed H4K16ac via modulation of TIP60

Next, we explored the acetylase which is responsible for H4 acetylation. TIP60, a histone acetyltransferase, is a key modulator in H4K16 acetylation [17]. Fig. 5A–D showed that, when ERK1/2 signaling was activated by transfection with pEGFP-Ras$^{G12V/T35S}$, expression levels of Sirt2 were unchanged, but the exogenous and endogenetic levels of TIP60 protein were dramatically reduced ($P < 0.05$). Besides that, SCH772984 could remarkably increase TIP60 expression ($P < 0.05$, Fig. 5E). Thus, activation of ERK1/2 pathway inhibited TIP60 expression post-transcriptionally. ChIP results from Fig. 5F showed that, the enrichment of TIP60 was significantly declined by the promoter of

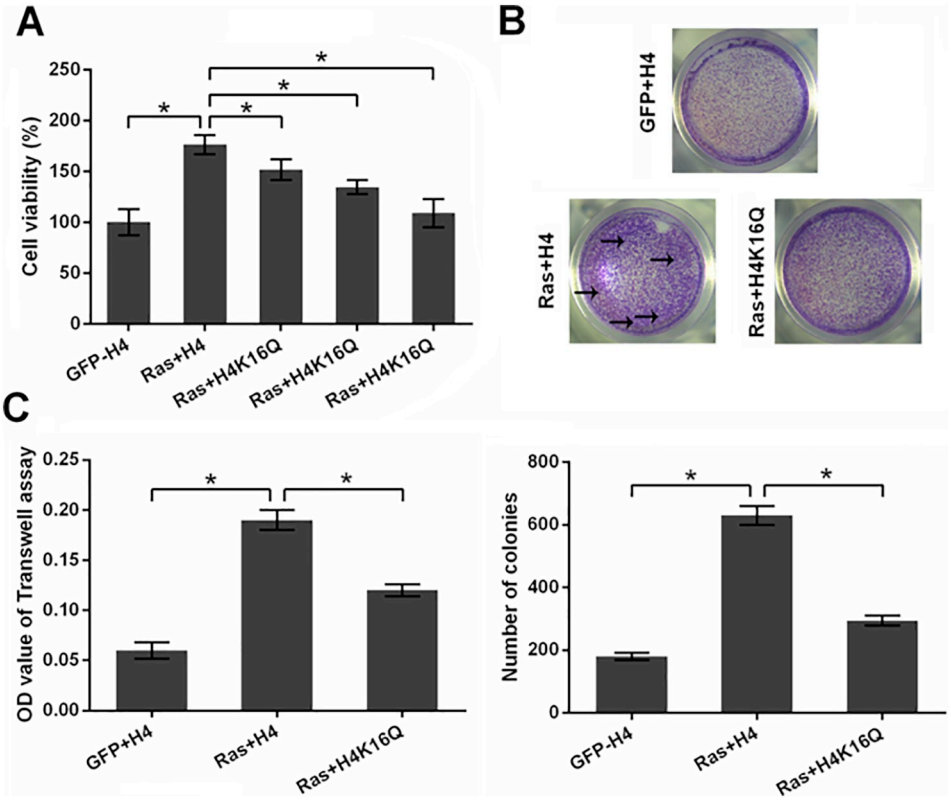

Fig. 2. H4K16ac inhibits A172 cells survival and migration. (A) A172 cells viability was gradually reduced by transfection with increasing amounts (0.5, 1, and 2 g) of H4K16Q, a plasmid for expressing mimicked H4K16ac. (B) Colony formation and (C) relative migration were both reduced by H4K16Q (2 g) transfection. *, $P < 0.05$ vs. the indicated group.

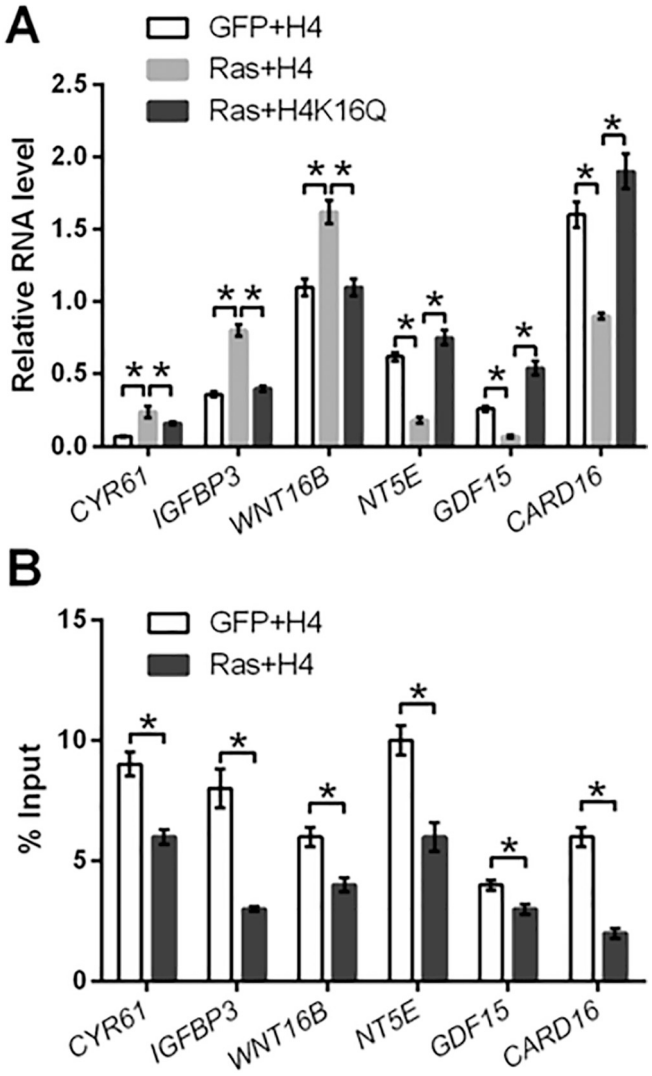

Fig. 3. H4K16ac participates in regulating ERK1/2 pathway downstream genes. (A) mRNA levels of *CYR61*, *IGFBP3* and *WNT16B* were down-regulated, whereas mRNA levels of *NT5E*, *GDF15* and *CARD16* were up-regulated by transfection with H4K16Q. (B) The enrichment of H4K16ac was significantly declined by the promoter of these genes. *, $P < 0.05$ vs. the indicated group.

ERK1/2 pathway downstream genes ($P < 0.05$), indicating TIP60 could also participate in regulating the transcription of ERK1/2 pathway downstream genes. Next, MG132, a potent proteasome inhibitor, was added into cell to reveal whether KRas-ERK1/2 activation regulated the acetylation of H4 at K16 via TIP60. Fig. 5G showed that, pEGFP-Ras$^{G12V/T35S}$ did not suppressed TIP60 protein expression when MG132 was added ($P > 0.05$). Fig. 5H–I displayed that, the inhibited expression of H4K16ac by transfection with pEGFP-Ras$^{G12V/T35S}$ could be reversed by addition of MG132 ($P < 0.05$). Therefore, it is rational that KRas-ERK1/2 signaling repressed H4K16ac via a proteasome-dependent manner.

Considering the important role of TIP60 in regulating H4K16ac expression, the effect of TIP60 in A172 cells survival and migration was studied. To this end, the expression of TIP60 in A172 cells was over-expressed by transfection with a TIP60 expressing plasmid (pc-TIP60). Transfection efficiency results were displayed in Fig. 6A. More interestingly, we found that transfection of cells with pc-TIP6 significantly suppressed A172 cells survival and migratory capacity ($P < 0.05$, Fig. 6B–C) as compared to transfection with an empty pcDNA-3.1 vector.

3.6. KRas-ERK1/2 signaling modulated TIP60 degeneration via MDM2

Acetylation of lys on histone proteins is often involved in the regulation of MDM2 [18]. Thereby, we focused on MDM2 for further investigating how KRas-ERK1/2 signaling degenerated TIP60. Results in Fig. 7A–B showed that, the exogenous and endogenetic levels of TIP60 protein were gradually repressed by MDM2 overexpression ($P < 0.05$). However, such decreased expression of TIP60 protein was not observed in cell transfected with a vector for expression of mutant type of MDM2 (Fig. 7C–D). Moreover, activation of ERK1/2 signaling induced by pEGFP-Ras$^{G12V/T35S}$ transfection could suppress MDM2 protein expression ($P < 0.05$, Fig. 7E). Silencing MDM2 expression by using siRNA transfection resulted in an up-regulated H4K16ac expression, even when KRas-ERK1/2 was activated ($P < 0.05$, Fig. 7F–G). A preliminary conclusion could be draw from these results, that KRas-ERK1/2 signaling inhibited the acetylation of H4 at K16 via MDM2-dependnet degeneration of TIP60.

4. Discussion

Histone modification is a regulatory mechanism that modulates the chromatin structure and thereby participates in regulating basic cellular functions, including cell cycle progression, cell growth and apoptosis [11]. Based on these reasons, researchers have recently focused on investigating the potential usage of histone modification in treating human cancers. This here, we aimed to reveal the cross-regulation between KRas-ERK1/2 signaling and H4K16 acetylation, in order to see whether KRas-ERK1/2 signaling participates in the onset and progression of glioma through modulation of H4K16ac. By conducting western blot analysis, H4K16ac was found to be deacetylated by KRas-ERK1/2 activation. Functional assays results showed that, H4K16ac could repress human glioblastoma A172 cells viability, colony formation and migratory capacity. Besides, H4K16ac is capable of regulating the transcription of several ERK1/2 pathway downstream genes. And also, KRas-ERK1/2 signaling deacetylated H4K16ac possibly via Sirt2 and MDM2-dependnet degeneration of TIP60.

H4K16ac is a highly abundant activating modification, with approximately 80% of H4 molecules having an acetyl group on K16 [19]. In mammals, H4K16ac is down-regulated in response to the defective DNA damage response (DDR). Inhibition of H4K16ac deacetylation will impede DDR, and H4K16ac is critical in DNA repair following double-strand break [20]. More importantly, recent papers demonstrated that H4K16ac was low expressed in various tumors. For instance, the expression level of H4K16ac in benign papilloma cells, squamous carcinoma cells and spindle cell carcinoma cells was much lower than that in normal skin cells [14]. The down-regulation of H4K16ac was also reported in other types of cancers, including gastric cancer [21], kidney cancer [22], breast cancer and medulloblastoma [23]. Besides, these examples indicated that deacetylation of H4K16ac appeared early and accumulated during the tumorigenic process, indicating H4K16ac as a key regulator in modulating the initiation and progression of cancers. However, the underlying mechanisms of the loss of H4K16ac expression is still a mystery. The present study revealed that, H4K16ac was significantly down-regulated in A172 cells following activation of KRas-ERK signaling. This finding provided a possibility that, the loss expression of H4K16ac in tumor cells owing to the activated KRas-ERK signaling. Our finding was similar with a previous study in which H4K16ac has been reported as a downstream target of Notch signaling in human hepatocellular carcinoma and breast cancer [15].

Unlimited proliferation capacity is one of the main reasons that responding for the incurable of glioma. In addition to the infinite proliferation, the metastatic potential of glioma is another major challenge for the management of this cancer, which leads to the high rates of recurrence and poor prognosis. Therefore, controlling of tumor cells proliferation and migration represents an important therapeutic target in the treatment of glioma. However, the present therapeutic strategies

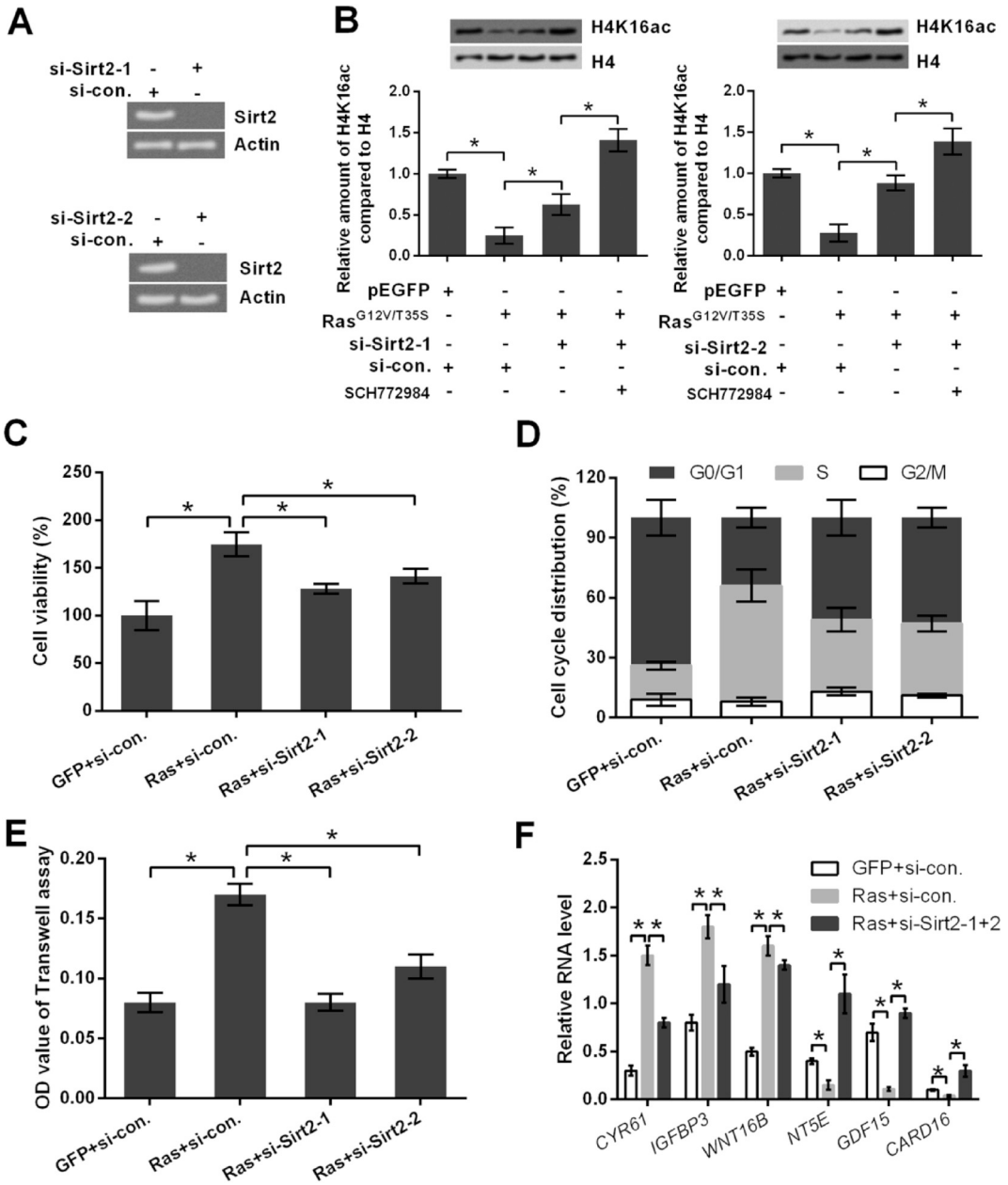

Fig. 4. KRas-ERK1/2 signaling represses H4K16ac via modulation of Sirt2. (A) Silence of Sirt2 by transfection with two sequences of siRNAs (si-Sirt2-1 and si-Sirt2-2). (B) Transfection of A172 cells with si-Sirt2-1 and si-Sirt2-2 recovered H4K16ac protein expression which was repressed by KRas-ERK1/2 activation. (C) Cell viability, (D) cell cycle progression, (E) relative migration, and (F) aberrant expression of ERK1/2 pathway downstream genes were all suppressed by transfection with Sirt2 siRNAs. *, $P < 0.05$ vs. the indicated group.

are limited in the view of neural toxicity, hematologic toxicity and the difficulty of drugs in crossing the blood-brain barrier. Only a fraction of studies have focused on evaluating the potential usage of histone modification in glioma treatment [24–26]. Herein, we demonstrated that transfection of A172 cells with H4K16Q construct (a plasmid for mimicking H4K16ac) significantly attenuated KRas-ERK1/2 activation induced growth and migration. This finding suggested the tumor-suppressive effects of H4K16ac on A172 cells, and provided an explanation for how KRas-ERK1/2 drives the initiation and progression of human cancers. Moreover, RT-PCR and ChIP assay results showed that, H4K16ac could regulate the transcription of *CYR61*, *IGFBP3*, *WNT16B*, *NT5E*, *GDF15* and *CARD16*. These six genes are all tumor-associated factors, and the downstream genes of KRas-ERK1/2 signaling as well. The transcriptionally regulated expression of these genes by H4K16ac further linked H4K16ac with the growth and migration of glioma cancer cells.

In order to further reveal how KRas-ERK1/2 signaling regulated the deacetylation of H4K16ac, the enzymes participating in the deacetylation of H4K16ac were studied. Histone deacetylases (HDACs) are well-known enzymes in catalyzing deacetylation. Depending on the homology to yeast HDACs, HDACs can be divided into four classes: HDAC I (HDAC1, 2, 3, 8), HDAC II (HDAC4, 5, 6, 7, 9, 10), HDAC III (Sirt1-Sirt7) and HDAC IV (HDAC11). Considering Sirt2 acts as a tumor suppressor in suppressing glioma cells growth [27–29], and previous study has shown a strong preference of Sirt2 for H4K16ac deacetylation [16], we investigated whether Sirt2 was responsible for H4K16ac deacetylation in A172 cells following KRas-ERK1/2 activation. As expected, our data showed that KRas-ERK1/2 signaling repressed H4 acetylation at K16 possibly via modulation of Sirt2. Besides, it seems that H4K16ac conferred its anti-proliferative and anti-migratory

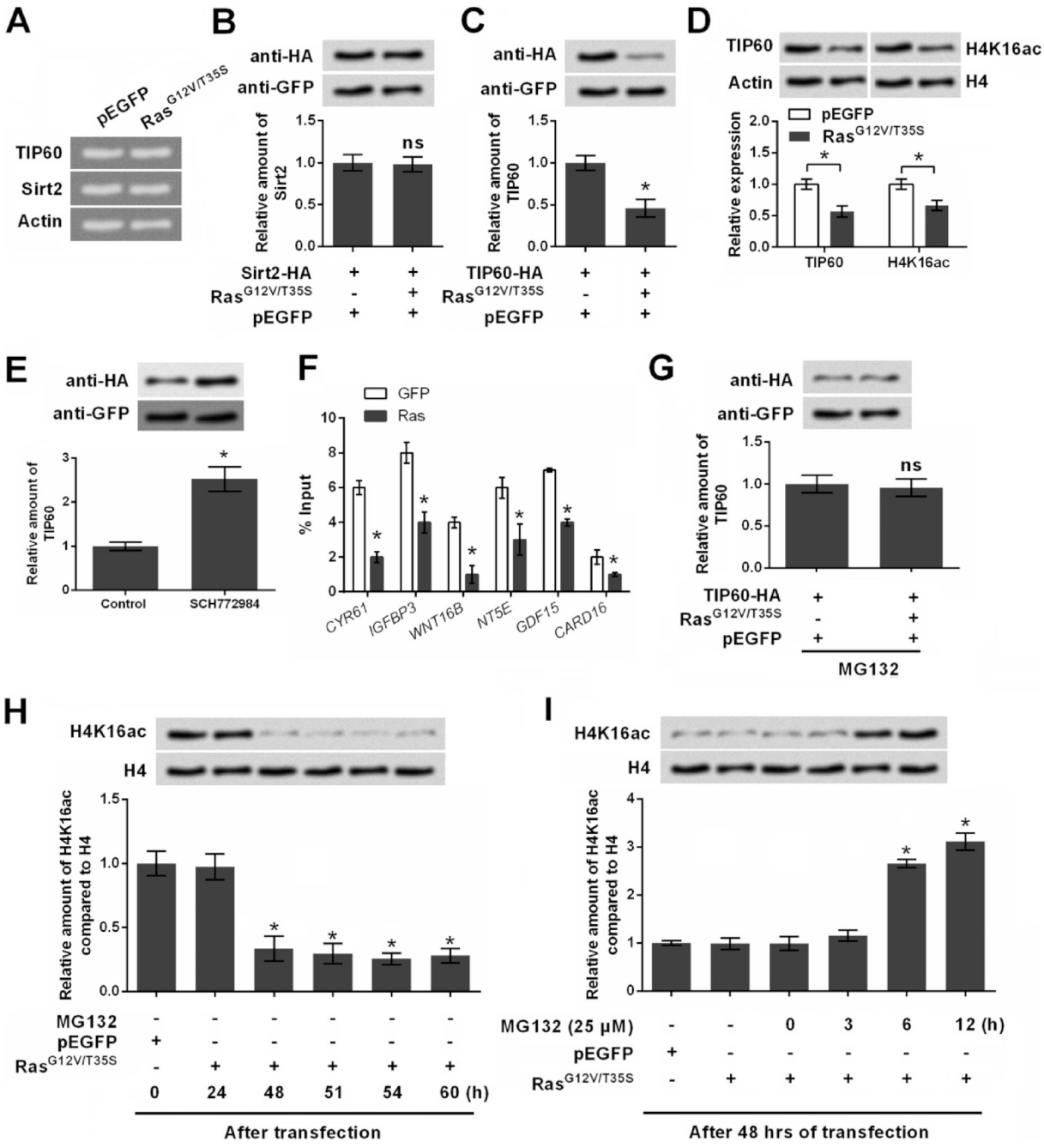

Fig. 5. KRas-ERK1/2 signaling represses H4K16ac via modulation of TIP60. (A) Pre-transcriptional expression of TIP60 and Sirt2, as well as (B) post-transcriptional expression of Sirt2 were unchanged by pEGFP-Ras$^{G12V/T35S}$ transfection. (C) Exogenous and (D) endogenetic expression of TIP60 protein was suppressed by pEGFP-Ras$^{G12V/T35S}$ transfection. (E) TIP60 expression was increased by SCH772984. (F) The enrichment of TIP60 was declined by the promoter of ERK1/2 pathway downstream genes. (G) MG132, a potent proteasome inhibitor, recovered TIP60 expression, which was down-regulated by pEGFP-Ras$^{G12V/T35S}$ transfection. (H) The accumulation of H4K16ac was gradually declined with the increasing time following pEGFP-Ras$^{G12V/T35S}$ transfection. (I) MG132 recovered H4K16ac expression even in pEGFP-Ras$^{G12V/T35S}$-transfected cell. ns, no significance. *, $P < 0.05$ vs. the indicated group.

properties might be through inhibiting the activity of Sirt2. However, further experiments are required to confirm this hypothesis.

Meanwhile, the enzymes which are in change of catalyzing H4K16 acetylation were investigated. MYST is one subfamily of histone acetyltransferases (HATs), containing four members, i.e., MOZ, Ybf2/Sas3, Sas2 and TIP60. Among which, TIP60 is a key enzyme in acetylating H2A at K5, H3 at K14, as well as H4 at K5, 8, 12 and 16. In the current study, H4K16 acetylation was found to be mediated by TIP60, which was confirmed the findings elsewhere described [17]. More interestingly, we found that KRas-ERK1/2 activation post-transcriptionally inhibited TIP60 expression. This finding implied that KRas-ERK1/2 inhibited H4K16 acetylation via down-regulating protein levels of TIP60. Besides, by adding with a potent proteasome inhibitor (MG132) into A172 cells, the repressed expression of TIP60 by KRas-ERK1/2 was recovered, indicating KRas-ERK1/2 inhibited TIP60 expression via a proteasome-dependent manner. Besides, the proteasome-dependent degradation of TIP60 was via modulation of MDM2, which was in line with a previous study [30].

In conclusion, our results suggest that activation of KRas-ERK signaling participates in the onset and progression of glioma at least partially through modulating acetylation of H4 at K16. KRas-ERK1/2 signaling mediates the acetylation of H4K16 possibly via Sirt2 and

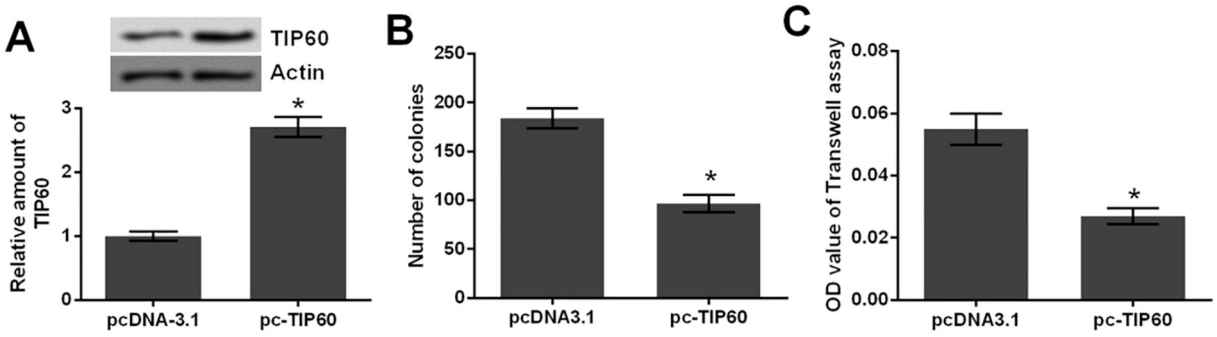

Fig. 6. TIP60 overexpression suppresses A172 cells survival and migration. (A) Expression of TIP60 in A172 cells was overexpressed by transfection with pc-TIP60, a plasmid for expressing TIP60. (B) Colony capacity and (C) relative migration were both suppressed by transfection with pc-TIP60. *, $P < 0.05$ vs. the indicated control group.

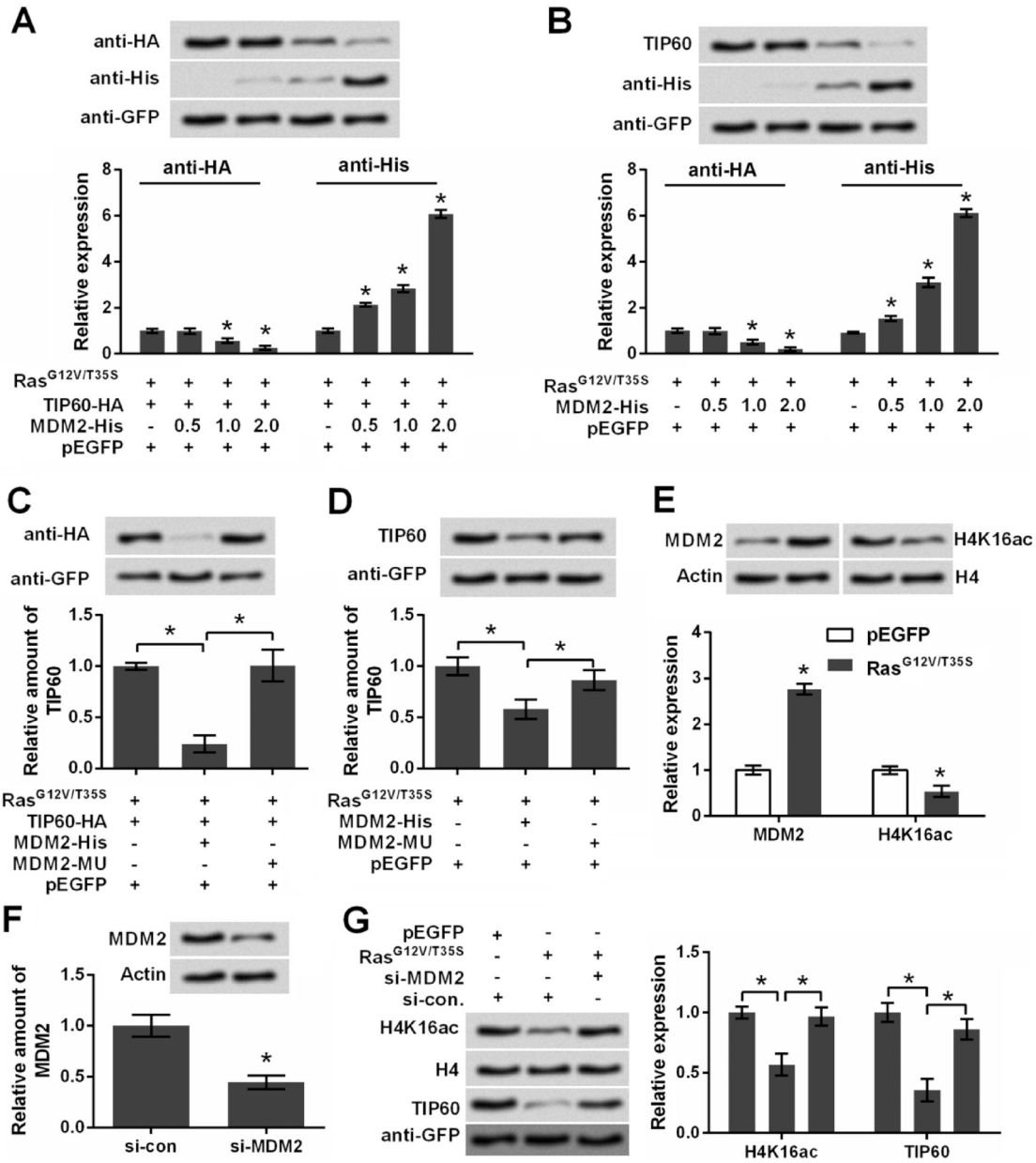

Fig. 7. KRas-ERK1/2 signaling modulates TIP60 degeneration via MDM2. (A) Exogenous and (B) endogenetic expression of TIP60 protein was gradually repressed by transfection with increasing amounts of MDM2 expression vector (MDM2-His). (C-D) No such down-regulations of TIP60 were observed after transfection with a vector for expression of mutant type of MDM2 (MDM2-MU). (E) pEGFP-Ras$^{G12V/T35S}$ transfection suppressed MDM2 expression. (F) Silence of MDM2 by using siRNA transfection. (G) MDM2 silence recovered H4K16ac expression even in pEGFP-Ras$^{G12V/T35S}$-transfected cell. *, $P < 0.05$ vs. the indicated group.

MDM2-dependnet degeneration of TIP60. These findings will provide a better understanding of KRas-ERK1/2 in human cancers.

Acknowledgements

None.

Funding

This research was supported by Shandong Medical and Health Technology Development Project in 2018 (No.2018WS476).

Conflict of interest

The authors declare no conflict of interest.

Author contributions

Conceived and designed the experiments: Yuzhen Wei, Fang Wang and Dongxu Yang;

Performed the experiments and analyzed the data: Yuzhen Wei, Fang Wang and Ben Sang; Contributed reagents/materials/analysis tools: Zhen Xu; Wrote the manuscript: Yuzhen Wei and Fang Wang; Revised the manuscript: Dongxu Yang.

References

[1] M.L. Goodenberger, R.B. Jenkins, Genetics of adult glioma, Cancer Genet. 205 (2012) 613–621.
[2] M. Houshyari, F. Hajalikhani, A. Rakhsha, P. Hajian, A comparative study of survival rate in high grade glioma tumors being treated by radiotherapy alone versus chemoradiation with nitrosourea, Global J. Health Sci. 7 (2015) 33–38.
[3] A. Omuro, L.M. DeAngelis, Glioblastoma and other malignant gliomas: a clinical review, JAMA 310 (2013) 1842–1850.
[4] K. Aldape, K.M. Brindle, L. Chesler, R. Chopra, A. Gajjar, M.R. Gilbert, N. Gottardo, D.H. Gutmann, D. Hargrave, E.C. Holland, D.T.W. Jones, J.A. Joyce, P. Kearns, M.W. Kieran, I.K. Mellinghoff, M. Merchant, S.M. Pfister, S.M. Pollard, V. Ramaswamy, Challenges to Curing Primary Brain Tumours, (2019).
[5] C.B. Knobbe, J. Reifenberger, G. Reifenberger, Mutation analysis of the Ras pathway genes NRAS, HRAS, KRAS and BRAF in glioblastomas, Acta Neuropathol. 108 (2004) 467–470.
[6] I.A. Prior, P.D. Lewis, C. Mattos, A comprehensive survey of Ras mutations in cancer, Cancer Res. 72 (2012) 2457–2467.
[7] F. Sanchez-Vega, M. Mina, J. Armenia, W.K. Chatila, A. Luna, K.C. La, S. Dimitriadoy, D.L. Liu, H.S. Kantheti, S. Saghafinia, D. Chakravarty, F. Daian, Q. Gao, M.H. Bailey, W.W. Liang, S.M. Foltz, I. Shmulevich, L. Ding, Z. Heins, A. Ochoa, B. Gross, J. Gao, H. Zhang, R. Kundra, C. Kandoth, I. Bahceci, L. Dervishi, U. Dogrusoz, W. Zhou, H. Shen, P.W. Laird, G.P. Way, C.S. Greene, H. Liang, Y. Xiao, C. Wang, A. Iavarone, A.H. Berger, T.G. Bivona, A.J. Lazar, G.D. Hammer, T. Giordano, L.N. Kwong, G. McArthur, C. Huang, A.D. Tward, M.J. Frederick, F. McCormick, M. Meyerson, E.M. Van Allen, A.D. Cherniack, G. Ciriello, C. Sander, N. Schultz, Oncogenic signaling pathways in the cancer genome atlas, Cell 173 (2018) 321–337 (e10).
[8] S.P. Mo, J.M. Coulson, I.A. Prior, RAS Variant Signalling, 46 (2018), pp. 1325–1332.
[9] L. Uhrbom, C. Dai, J.C. Celestino, M.K. Rosenblum, G.N. Fuller, E.C. Holland, Ink4a-Arf loss cooperates with KRas activation in astrocytes and neural progenitors to generate glioblastomas of various morphologies depending on activated Akt, Cancer Res. 62 (2002) 5551–5558.
[10] D.P. Potaczek, H. Harb, S. Michel, B.A. Alhamwe, H. Renz, J. Tost, Epigenetics and allergy: from basic mechanisms to clinical applications, Epigenomics 9 (2017) 539–571.
[11] R. Wang, M. Xin, Y. Li, P. Zhang, M. Zhang, The functions of histone modification enzymes in cancer, Curr. Protein Pept. Sci. 17 (2016) 438–445.
[12] K. Rifai, G. Judes, M. Idrissou, M. Daures, Y.J. Bignon, F. Penault-Llorca, D. Bernard-Gallon, SIRT1-dependent epigenetic regulation of H3 and H4 histone acetylation in human breast cancer, Oncotarget 9 (2018) 30661–30678.
[13] Z. Wang, C. Zang, J.A. Rosenfeld, D.E. Schones, A. Barski, S. Cuddapah, K. Cui, T.Y. Roh, W. Peng, M.Q. Zhang, K. Zhao, Combinatorial patterns of histone acetylations and methylations in the human genome, Nat. Genet. 40 (2008) 897–903.
[14] M.F. Fraga, E. Ballestar, A. Villar-Garea, M. Boix-Chornet, J. Espada, G. Schotta, T. Bonaldi, C. Haydon, S. Ropero, K. Petrie, N.G. Iyer, A. Perez-Rosado, E. Calvo, J.A. Lopez, A. Cano, M.J. Calasanz, D. Colomer, M.A. Piris, N. Ahn, A. Imhof, C. Caldas, T. Jenuwein, M. Esteller, Loss of acetylation at Lys16 and trimethylation at Lys20 of histone H4 is a common hallmark of human cancer, Nat. Genet. 37 (2005) 391–400.
[15] Y. Liu, Z.B. Xing, S.Q. Wang, S. Chen, Y.K. Liu, Y.H. Li, Y.F. Li, Y.Q. Wang, Y. Lu, W.N. Hu, J.H. Zhang, MDM2-MOF-H4K16ac axis contributes to tumorigenesis induced by Notch, FEBS J. 281 (2014) 3315–3324.
[16] A. Vaquero, M.B. Scher, D.H. Lee, A. Sutton, H.L. Cheng, F.W. Alt, L. Serrano, R. Sternglanz, D. Reinberg, SirT2 is a histone deacetylase with preference for histone H4 Lys 16 during mitosis, Genes Dev. 20 (2006) 1256–1261.
[17] L.M. Tam, J. Jiang, P. Wang, L. Li, W. Miao, X. Dong, Y. Wang, Arsenite Binds to the Zinc Finger Motif of TIP60 Histone Acetyltransferase and Induces Its Degradation via the 26S Proteasome, 30 (2017), pp. 1685–1693.
[18] N.T. Nihira, K. Ogura, K. Shimizu, Acetylation-dependent regulation of MDM2 E3 ligase activity dictates its oncogenic function, 10 (2017).
[19] C.M. Smith, P.R. Gafken, Z. Zhang, D.E. Gottschling, J.B. Smith, D.L. Smith, Mass spectrometric quantification of acetylation at specific lysines within the amino-terminal tail of histone H4, Anal. Biochem. 316 (2003) 23–33.
[20] G.G. Sharma, S. So, A. Gupta, R. Kumar, C. Cayrou, N. Avvakumov, U. Bhadra, R.K. Pandita, M.H. Porteus, D.J. Chen, J. Cote, T.K. Pandita, MOF and histone H4 acetylation at lysine 16 are critical for DNA damage response and double-strand break repair, Mol. Cell. Biol. 30 (2010) 3582–3595.
[21] L. Zhu, J. Yang, L. Zhao, X. Yu, L. Wang, F. Wang, Y. Cai, J. Jin, Expression of hMOF, but not HDAC4, is responsible for the global histone H4K16 acetylation in gastric carcinoma, Int. J. Oncol. 46 (2015) 2535–2545.
[22] Y. Wang, R. Zhang, D. Wu, Z. Lu, W. Sun, Y. Cai, C. Wang, J. Jin, Epigenetic change in kidney tumor: downregulation of histone acetyltransferase MYST1 in human renal cell carcinoma, J. Exp. Clin. Cancer Res. 32 (2013) 8.
[23] S. Pfister, S. Rea, M. Taipale, F. Mendrzyk, B. Straub, C. Ittrich, O. Thuerigen, H.P. Sinn, A. Akhtar, P. Lichter, The histone acetyltransferase hMOF is frequently downregulated in primary breast carcinoma and medulloblastoma and constitutes a biomarker for clinical outcome in medulloblastoma, Int. J. Cancer 122 (2008) 1207–1213.
[24] B. Tung, D. Ma, S. Wang, O. Oyinlade, J. Laterra, M. Ying, S.Q. Lv, S. Wei, S. Xia, Kruppel-like Factor 9 and Histone Deacetylase Inhibitors Synergistically Induce Cell Death in Glioblastoma Stem-like Cells, 18 (2018), p. 1025.
[25] S.A. Choi, C. Lee, P.A. Kwak, C.K. Park, K.C. Wang, J.H. Phi, J.Y. Lee, S. Chong, S.K. Kim, Histone deacetylase inhibitor panobinostat potentiates the anti-cancer effects of mesenchymal stem cell-based sTRAIL gene therapy against malignant glioma, Cancer Lett. 442 (2018) 161–169.
[26] I.A. Ciechomska, M.P. Marciniak, J. Jackl, B. Kaminska, Pre-treatment or post-treatment of human glioma cells with BIX01294, the inhibitor of histone methyltransferase G9a, sensitizes cells to temozolomide, Front. Pharmacol. 9 (2018) 1271.
[27] Y. Li, D. Dai, Q. Lu, M. Fei, M. Li, X. Wu, Sirt2 suppresses glioma cell growth through targeting NF-kappaB-miR-21 axis, Biochem. Biophys. Res. Commun. 441 (2013) 661–667.
[28] S. Sayd, C. Thirant, E.A. El-Habr, J. Lipecka, L.G. Dubois, A. Bogeas, N. Tahiri-Jouti, H. Chneiweiss, M.P. Junier, Sirtuin-2 activity is required for glioma stem cell proliferation arrest but not necrosis induced by resveratrol, Stem Cell Rev. 10 (2014) 103–113.
[29] X. He, H. Nie, Y. Hong, C. Sheng, W. Xia, W. Ying, SIRT2 activity is required for the survival of C6 glioma cells, Biochem. Biophys. Res. Commun. 417 (2012) 468–472.
[30] G. Legube, L.K. Linares, C. Lemercier, M. Scheffner, S. Khochbin, D. Trouche, Tip60 is targeted to proteasome-mediated degradation by Mdm2 and accumulates after UV irradiation, EMBO J. 21 (2002) 1704–1712.